

ELECTRON LINACS*

Gregory A. Loew
Stanford Linear Accelerator Center
Stanford University, Stanford, California 94305

Summary

To study the present status of the thousand or so electron linacs in the world, and future trends in the field, we have classified these machines according to their use: medical, industrial, and nuclear physics. In the medical category, two types of electron linacs are discussed: the conventional ones which are used for X-ray and electron therapy, and those which may in the future be used for negative pion therapy. The section on industrial machines includes linacs for radiographic and other specialized applications. In the nuclear physics category, the status of conventional low- and medium-energy as well as high duty cycle linacs is reviewed. The question of how one might obtain a C.W., 1 GeV, 100 μ A electron linac is raised and various options using recirculation and stretchers are examined. In this connection, the status of RF superconductivity is summarized. Following, there is a review of linacs for injectors into synchrotrons and e^\pm storage rings. The paper ends with a description of recent work done to upgrade the only multi-GeV linac, namely SLAC.

Introduction

This paper concerns itself with linear electron accelerators in which the electrons (or positrons) acquire their kinetic energy from some type of RF power source. Electrostatic accelerators such as Van de Graaffs, induction linacs, and other machines will not be covered here.

In the past forty years, since the inception of the first modern electron linacs in England and at Stanford in the USA, both the number and the diversity of these machines have expanded enormously. Today there are close to 1000 electron linacs in the world. The evolution of designs has been governed by both supply and demand, namely, self-motivated progress on the part of accelerator builders and improvements generated by the needs of the users and the financial means at their disposal. Considerable progress has also been realized because of developments in adjoining branches of technology such as metallurgy, vacuum, magnet design and, above all, electronic instrumentation which has made possible increased compactness, flexibility of use, and speed of control.

While there are many ways in which the field can be surveyed, in this paper we shall review status, innovations and future trends by categorizing electron linacs according to their use: medical, industrial, and nuclear physics. In this latter class, we shall distinguish conventional low- and medium-energy linacs of various characteristics, special high duty cycle machines (≤ 1 GeV), injectors into synchrotrons and e^\pm storage rings, and multi-GeV accelerators (SLAC). In looking at the future, we shall consider how one might attain the goal of a C.W., 1 GeV, 100 μ A machine by means of beam recirculation, stretching and/or RF superconductivity.

I. Electron Linacs for Radiotherapy

a. X-ray and Electron Therapy

Electron linacs began to come into use for radio-

therapy in 1953 with the inception of an 8 MeV machine at the Hammersmith Hospital in London, England. They can now be found in several hundred hospitals all over the world. Therapy is performed either with X-rays (derived from the primary electrons hitting a target) or with the primary electrons themselves. While the machines on the market are of many different types and offer a wide variety of features, they can be classified into two broad categories: (i) linacs with electron energies below 10 MeV which are almost exclusively used for X-ray therapy, and (ii) linacs with energies between 10 and 35 MeV which offer both options, i.e., X-rays generated by an electron beam at one or two discrete energies, and electrons at several discrete energies ranging all the way up to maximum capability. Since, for a given dose, the biological effect of X-rays and electrons is believed to be indistinguishable, deciding between X-ray therapy (~90% of all treatments) and electron therapy (~10%) in a hospital which has both modalities available is entirely determined by the type of tumor and the optimum dose distribution that can be delivered to it. The criteria are complex but can be understood in a general manner by referring to Fig. 1 from Ref. 1. It is seen that electrons

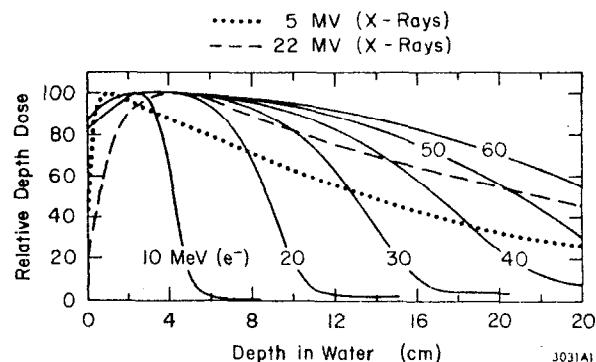


Fig. 1--Relative depth-dose curves for electrons (at 200 cm source-to-skin distance) and X-rays (at 100 cm target-to-skin distance) as a function of depth in water (large field, central axis).

between 10 and 35 MeV have relatively sharp and well-defined dose dropoffs but suffer from the disadvantage of high entrance dose at the skin. X-rays on the other hand exhibit a much lower entrance dose but a much broader depth distribution, which results in a less favorable concentration but also in a reduced risk for error. Since sparing of the skin is of vital importance (unless of course cancer of the skin itself is involved), X-ray therapy is chosen in a great majority of cases. Electron therapy, however, is desirable in specific cases for deep tumors, so-called "booster" doses (added on to X-ray therapy), and skin cancer.

Table I gives a list² of commercially available or announced radiotherapy electron linacs and some of their characteristics. Practically all these machines have an

*Work supported by the Energy Research and Development Administration.

Table I: Commercially available or announced radiotherapy electron linacs.

Manufacturer	Model	Beam Energy and Type of Radiation	Accelerator Structure Length and Type	Microwave Power Source	Bending Angle of Magnet	X-ray Field Size at SAD or SSD
CGR/AECL	Therac 6	6 MV X-rays	1.0 m TW	2 MW magnetron	$\sim 270^\circ$	40 x 40 cm
	Therac 20	18 MV X-rays 6-20 MeV electrons	2.3 m TW	5 MW klystron	$\sim 270^\circ$	40 x 40 cm
	Therac 40	25 MV X-rays 7-32 MeV electrons	6.0 m TW 2 sections	9 MW klystron	$+30^\circ, -30^\circ$ $+30^\circ, -120^\circ$	not given
Mitsubishi	ML-4M	4 MV X-rays	0.21 m SW	2 MW magnetron	none	
	ML-15 MIB	10 MV X-rays 8-15 MeV electrons	1.7 m TW	5 MW klystron	$\sim 90^\circ$	30 x 30 cm
Philips/MEL	SL75-5	4-6 MV X-rays	1.25 m TW	2 MW magnetron	$\sim 90^\circ$	40 x 40 cm
	SL75-10	8 MV X-rays 4-10 MeV electrons	2.25 m TW	2 MW magnetron	$\sim 90^\circ$	30 x 30 cm
	SL75-20	8 and 16 MV X-rays 5-20 MeV electrons	2.5 m TW	5 MW magnetron	$\sim 90^\circ$	30 x 30 cm
Radiation Dynamics	Dynaray 4	3-5 MV X-rays	0.75 m TW	2 MW magnetron	$\sim 90^\circ$	30 x 30 cm
	Dynaray 10	8 MV X-rays 4-10 MeV electrons	2.25 m TW	2 MW magnetron	266°	35 x 35 cm
	Dynaray 18	6-12 MV X-rays 6-18 MeV electrons	~ 2 m TW	5 MW klystron	266°	30 x 30 cm
SHM/FMI	Therapi 4	4 MV X-rays (no gantry rotation)	0.3 m SW	2 MW magnetron	none	40 x 40 cm
	Therapi 400	4 MV X-rays	0.3 m SW	2 MW magnetron	none	40 x 40 cm
Siemens/ARCO	Mevatron 6	6 MV X-rays	0.95 m SW	2 MW magnetron	261°	35 x 35 cm
	Mevatron 12	8 or 10 MV X-rays 3-11 MeV electrons	1.35 m SW	2 MW magnetron	261°	35 x 35 cm
	Mevatron 20	10 or 15 MV X-rays 3-18 MeV electrons	1.38 m SW	7 MW klystron	270°	35 x 35 cm
Toshiba	LMR-4	4 MV X-rays	0.31 m SW	2 MW magnetron	none	40 x 40 cm
	LMR-13	10 MV X-rays 8-13 MeV electrons	1.6 m TW	4.8 MW magnetron	105°	30 x 30 cm
	LMR-15	10 MV X-rays 8-16 MeV electrons	1.73 m TW	4.8 MW magnetron	105°	30 x 30 cm
Varian	Clinac 4	4 MV X-rays	0.3 m SW	2 MW magnetron	none	32 x 32 cm
	Clinac 6X	6 MV X-rays	0.3 m SW	2 MW magnetron	none	32 x 32 cm
	Clinac 12	6 or 8 MV X-rays 6-12 MeV electrons	1.0 m SW	2 MW magnetron	270°	35 x 35 cm
	Clinac 18	10 MV X-rays 6-18 MeV electrons	1.4 m SW	5 MW klystron	270°	35 x 35 cm
	Clinac 35	8 and 25 MV X-rays 7-28 MeV electrons	2.25 m TW	20 MW klystron	$\sim 57^\circ$ and 90°	35 x 35 cm

isocentric mount which enables the gantry to be rotated by at least 360° . The target or source-to-axis distance (SAD) is commonly of the order of 100 cm and the maximum source-to-skin (SSD) distance of the order of 120 cm. Within the fields given in the last column of Table I these linacs can now deliver between 300 and 500 rads/min. Figures 2 and 3 show cutaway views of two representative machines (Varian's CLINAC 6X and CLINAC 12). The first uses the "straight ahead" beam design characteristic of most of the smaller X-ray machines. The second uses an achromatic magnet system which bends and focuses the beam on target and must be adjusted for different electron beam energies. Discrete electron beam energies are obtained by a variety of adjustments such as magnetron or klystron output power or RF frequency. The RF power can be changed by adjusting the high voltage on the tube or the match on the three- or four-port circulator generally inserted between the tube and the accelerating guide for RF isolation. X-ray output can be reduced from its maximum value by reducing repetition rate. Typical duty cycles are of the order of 10^{-3} with RF pulse lengths between 2-3 μ s. Gun voltage is

in the range of 15-30 kV; it is generally adjusted to control capture and beam current in the electron mode. For X-rays, peak currents are typically between 100 and 200 mA. For electrons, they are reduced by a factor of 100. The frequency of most of these machines is either ~ 2856 MHz or ~ 2998 MHz and it is governed by the availability of reliable commercial tubes. AFC is generally necessary to preserve a good match to the accelerating guide. Impressive improvements have been made in the past few years in the shunt impedance of the standing-wave (SW) accelerating guide, commonly the side-coupled structure. Typical values at S-band for a standing-wave (SW) structure are of the order of 70 megohms/m but impedances in excess of 80 megohms/m have recently been reported.³

A typical treatment consists of delivering 6000 rads fractionated into about 30 equal daily increments of 200 rads each and it is desirable to control each dose to within 2%. Thus, not surprisingly, the most delicate features of these machines have to do with dose homogeneity, stability, and control. Leakage and so-called "penumbra" effects due to edge scattering must be

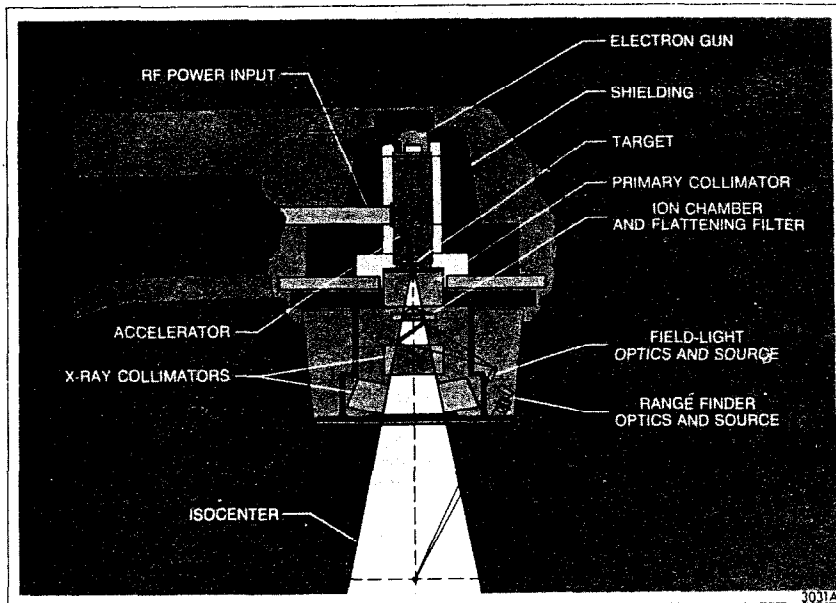


Fig. 2--Varian CLINAC 6X.

minimized. To achieve these features requires good energy stability, minimization of beam spot size and position changes at the target and well designed field flatteners. Energy stability in turn requires stable matching conditions which are not easy to achieve with imperfect RF sources and over wide beam current excursions, particularly with standing-wave structures. The more flexible the machine, the more difficult it is to meet all these criteria. It is in these areas that improvements remain to be made.

Another area where improvement is needed is cost. The smaller isocentric X-ray machines all seem to cost between \$150,000 and \$250,000 and generally can be

afforded by an average hospital. On the other hand, some of the higher energy electron machines cost between $\frac{1}{2}$ and $1\frac{1}{2}$ million dollars and they are comparatively more complex to use. Their price is relatively high to be widely affordable, given the fact that the number of patients that can be treated per day with these higher energy machines is often lower. A challenge to the accelerator community would be to build a machine with two possible X-ray outputs (4 and 20 MV) and a continuous range of electron energies between 5 and 30 MeV for less than \$400,000!

b. Electron Linacs for Pion Therapy

Another challenge to the electron linac designer now comes from the medical community's interest in negative pion therapy. The potentialities of negative pion therapy have been explored by a number of authors and a successful prototype for a superconducting pion concentrator (SMPG), for Stanford Medical Pion Generator) has been built at the W. W. Hansen Laboratories at Stanford University (for a review see,

for example, Ref. 4). In order to achieve the desired pion dose rate of 30 rad/min in a 1000 cc volume, it is necessary to bombard the primary target of such an SMPG with 6 kW of ~600 MeV protons or 300 kW of ~600 MeV electrons. At first glance this power ratio would seem to favor strongly the proton machines. A committee under J. P. Blewett in fact met in the summer of 1975 to examine the relative merits and costs of proton synchrotrons, proton linacs, and electron linacs to perform this task. The conclusions of the committee were that the proton linac may hold the best long range potential but that the electron linac is at the present time the simplest, cheapest, state-of-the-art candidate. General design considerations for proton linacs, electron linacs,

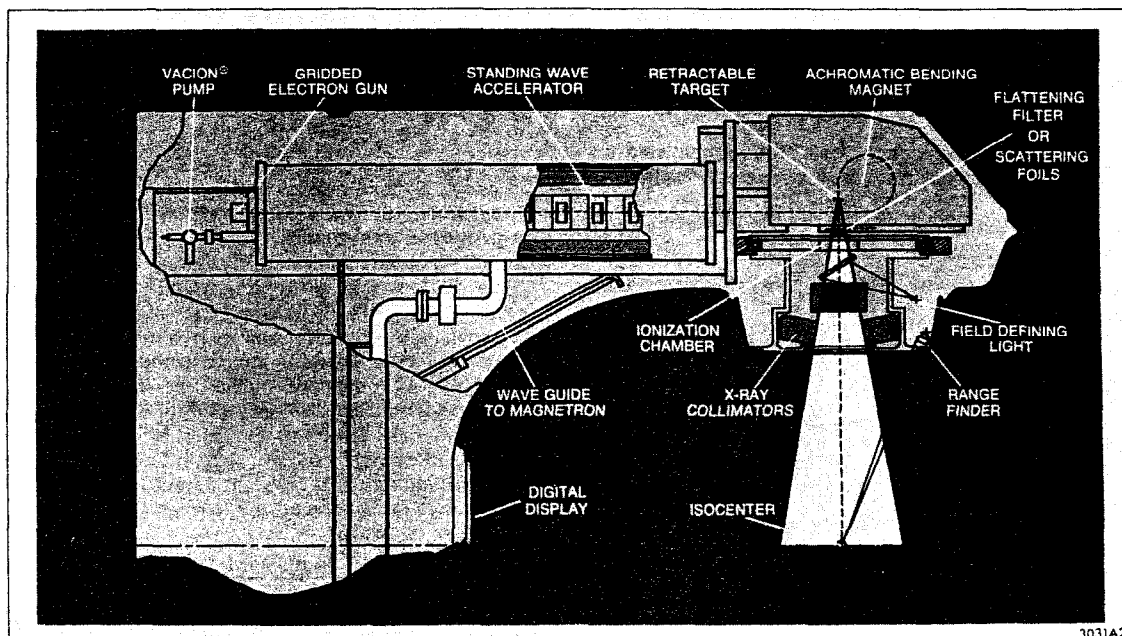


Fig. 3--Varian CLINAC 12.

and microtrons can be found in the literature.^{5,6,7} In response to a request from the Radiology Department of the Stanford Medical Center, SLAC came up with the design of a specific electron linac and associated beam transport system that could be built within a period of 2.5 years for about \$8 million.

The starting point to determine the main parameters of this machine was the pion yield vs incident electron energy obtained from experiments with the Stanford Mark III linac.⁸ A reasonable linear approximation of the form

$$N_{\pi}/\text{mA/sr}/1\%\Delta p/p = 4.125 \times 10^5 (V_{\text{MeV}} - 200) \quad (1)$$

seems valid between 300 and 900 MeV. Given that the desired number of pions out of the target has been established at $7.42 \times 10^7 \pi/\text{sr}/1\%\Delta p/p$, one can obtain a relationship between the necessary electron energy and current:

$$V_{\text{MeV}} - 200 = \frac{0.18}{i_{A, \text{pk}} D_b} \quad (2)$$

where $i_{A, \text{pk}}$ is the peak current in amperes and D_b is the beam duty cycle. The energy of a multisection constant-gradient linac is given by⁹

$$V = n(1 - e^{-2\tau})^{\frac{1}{2}} (Pr\ell)^{\frac{1}{2}} - \frac{i_{\text{pk}} r \ell n}{2} \left(1 - \frac{2\tau e^{-2\tau}}{1 - e^{-2\tau}} \right) \quad (3)$$

where P is the peak RF power into a section of length ℓ , attenuation τ , and shunt impedance r , n is the number of sections, and i_{pk} is the peak current. Combining Eqs. (2) and (3), we get expression (4)

$$n(1 - e^{-2\tau})^{\frac{1}{2}} (Pr\ell)^{\frac{1}{2}} - 200 - \frac{n i_{\text{pk}} r \ell}{2} \left(1 - \frac{2\tau e^{-2\tau}}{1 - e^{-2\tau}} \right) = \frac{0.18}{D_b i_{\text{pk}}} \quad (4)$$

which together with the expression for RF-to-beam power conversion efficiency

$$\eta = \frac{i_{\text{pk}} V D_b}{n P D_{\text{RF}}} \quad (5)$$

where D_{RF} is the RF duty cycle, can be programmed on a computer and used to optimize any practical design.

Criteria for a practical design can be somewhat subjective but should include:

- A commercially available, reliable, reasonably priced klystron
- Minimization of total accelerator length and RF power
- Practical RF pulse length
- Minimization of risk of beam breakup
- Overall economy

A large number of S-band and L-band designs were explored with these criteria in mind and sets of curves such as those shown in Figs. 4a and 4b were obtained. From these it can be seen that the increase in pion yield with energy favors relatively higher values of τ and correspondingly lower peak beam currents which in turn are more conservative from the point of view of beam breakup. Although choosing L-band reduces the risk of beam

ASSUMPTIONS: $\ell = 3\text{m}$, $D_{\text{RF}} = 10^{-3}$, $r = 50 \text{ M}\Omega/\text{m}$,
 $P = 30 \text{ MW}$, $f = 2856 \text{ MHz}$

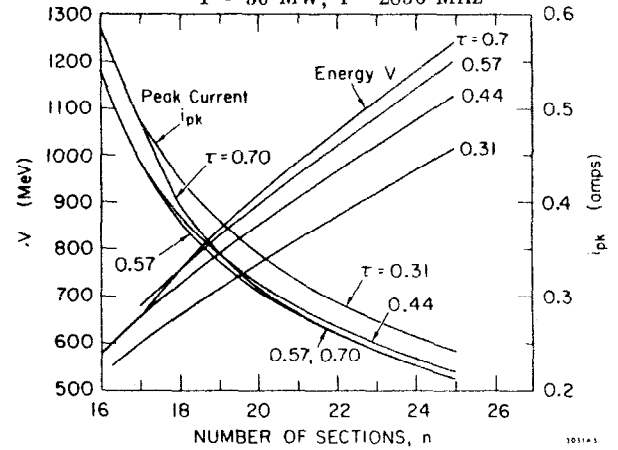


Fig. 4a--Energy V (MeV) and corresponding peak current i_{pk} (A) versus number of sections n for design accelerator capable of producing desired electron beam for pion generation.

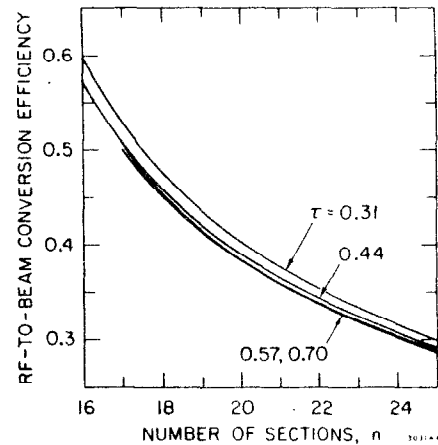


Fig. 4b--RF-to-beam conversion efficiency versus number of sections n .

breakup because the HEM_{11} -mode r/Q scales with frequency, S-band seems preferable because of shorter total length and/or lower total RF power. The parameters for a proposed design which makes use of readily fabricated SLAC-type sections and klystrons are given in Table II. This design is by no means unique but it should be practical and realizable without major surprises. With extra money, one could for example increase the number of sections from 18 to 20 and decrease τ somewhat. Calculations carried out at SLAC by R. H. Helm indicate that quadrupole focusing and detuning of the HEM_{11} resonance in the first two sections by about 2 MHz make the proposed design entirely safe from the point of view of beam breakup. An injector capable of launching a 0.350A beam into such an accelerator should be straightforward.

II. Industrial Electron Linacs

The class of electron linacs used for industrial purposes is not quite as well defined as that for radiotherapy because the boundary between industrial applications and

Table II: Parameters for proposed electron linac for pion radiotherapy.

Loaded electron energy V	770 MeV
No-load electron energy V ₀	1020 MeV
Beam loading voltage V _b	250 MeV
Peak electron current	0.350 A
Repetition rate	180 pps
RF pulse length t _{RF}	5.55 μs
Beam pulse length t _b	4.95 μs
Klystron output power P _{pk} (SLAC-RCA-ITT model)	30 MW
Power into accelerator section (allowing for waveguide losses)	28.5 MW
Frequency f	2856 MHz
Shunt impedance per unit length r	57 MΩ/m
Attenuation parameter r	0.57 nepers
Section length l	3 m
Number of klystrons and modulators	18
Number of accelerator sections n (including injector)	18
Number of instrumentation drift sections	8
Length of instrumentation drift sections	1.5 m
Number of quadrupole doublets	8
Total approximate length	75 m

pure nuclear research is often fuzzy. One application where industrial usage is clearly categorized is that of radiography. Table III gives a list of commercial models together with some of their specifications. Most of these machines use basic components very similar to the radiotherapy linacs. The electron beam, however, is never extracted and in most cases only one energy is used for

X-ray generation. The electron current is generally in the range of 100 to 200 mA with a duty cycle of 10⁻³. The machines are usually crane-mounted and they are built for heavy duty in a harsh environment.

Machines for other applied usages are more specialized and therefore require more particular beam specifications. Table IV lists some of the more modern machines, either in existence or under construction, with their applications and noteworthy characteristics. This list is of course only representative and certainly not all-inclusive.

Other applications include radiobiological research, pulse radiolysis, dosimetry, and sterilization. Among the older but noteworthy accelerators, one can list the L-band IRT, San Diego linac capable of 10A short pulses for research and sterilization, the L-band E.G. & G. / ERDA linac in Goleta, California, used for measurements of weapons test detectors and capable of accelerating a single bunch (30-50 picoseconds) by using a sub-harmonic buncher, and the US Army S-band, 10 MeV, 650 mA linac at Natick, Massachusetts, made by Varian in 1961, which in the past 12 months irradiated 30,000 kilograms of meat at -40°C to a dose of 4.5 megarads!

III. Electron Linacs for Nuclear Physics

a. Conventional Low- and Medium-Energy Machines

The machines in this category have been and are still the "work horses" used all over the world for nuclear physics research with electron beams. Table V gives a representative list of these accelerators with some of their parameters. Unless noted otherwise, they

Table III: Commercially available or announced electron linacs for industrial radiography.

Manufacturer	Model	Nominal Electron Energy (MeV)	Microwave Power Source	Maximum X-Ray Output (unflattened) (rad min ⁻¹ m ²)	Maximum Field Size (at 1 m) (cm)	Nominal photon Leakage Radiation (per cent of useful beam at 1 m)
CGR/AECL	Neptune 6	6	2 MW magnetron	750	50 (diam)	0.1
	Neptune 10	10	? magnetron	2000	50 (diam)	0.1
Mitsubishi	ML-1 RII	0.95	1 MW magnetron	20	30 (diam)	0.1
	ML-3R	1.5	1.5 MW magnetron	50	30 (diam)	0.3
	ML-5R	3	2 MW magnetron	300	30 (diam)	0.3
	ML-10R	8	2 MW magnetron	1500	30 (diam)	0.2
	ML-15RII	12	5 MW klystron	7000	30 (diam)	0.1
Radiation Dynamics	Super X 600	8	2 MW magnetron	600	30 (diam)	0.1
	Super X 2000	8	2 MW magnetron	2000	30 (diam)	0.1
	Super XX	12	5 MW klystron	6000	30 (diam)	0.1
SHM	Radiograf 4	4	2 MW magnetron	500	26 x 35	0.5
	Radiograf 13	13	2 MW magnetron	6000	26 x 35	0.5
Varian	Linatron 200	2	1 MW magnetron	175	77 x 77	0.02
	Linatron 400	4	2 MW magnetron	400	39 x 39	0.25
	Linatron 2000	8	2 MW magnetron	2000	55 (diam)	0.1
	Linatron 6000	15	5 MW klystron	6000	27 (diam)	0.1

Table IV: Selected list of recent electron linacs used for specialized applications.

Institution	Manufacturer and Year of Installation	Application	Energy	Length	Number and Type of Sections	Number and Type of Power Sources	Frequency	Maximum Beam Duty Cycle	Peak Current Range	Noteworthy Features
Argonne National Laboratory, Chicago, USA	ARCO 1970	Radiation chemistry Photoneutron physics	10-22 MeV	5.81 m	2 TW	2 klystrons 20 MW	1300.7 MHz	1.5×10^{-3}	1 mA to 2.5 A for 10 μ sec pulses 2 μ A to 22 A for 10 nsec pulses	Very short high current pulses Very low attenuation length ~ 0.11 Subharmonic bunching
BAM, Berlin, Germany	Radiation Dynamics 1973	γ -activation analysis Neutron-radiography Radiation protection	4-36 MeV	5 m	2 TW	1 klystron 20 MW	2856 MHz	1.2×10^{-3}	0-450 mA for 3.2 μ sec pulses	Flexible repetition rate between 12.5 and 300 pps
Euratom, Geel, Belgium	CORUMER construction	Neutron production for reactor research	100-150 MeV	15 m	1 SW, 2 TW	3 klystrons 13-18 MW	2994 MHz	2×10^{-3}	10-220 mA for 2 μ sec pulses 1.5 to 9 A for 4-100 nsec pulses	Flexible repetition rate between 250 and 900 pps Very short, high current pulses
National Physical Laboratory, Teddington, GB	Radiation Dynamics 1975	Radiation metrology	10-22 MeV	2 m	2 TW	1 klystron 20 MW	2856 MHz	0.7×10^{-3}	10^{-4} mA to 700 mA for 3 μ sec pulses 10-4 mA to 5 A for 5 nsec pulses	Flexible repetition rate (1-150 pps) Very short, high current pulses
RISO, Roskilde, Denmark	Halmeskov Research Corp. 1976	Radiation research	4.5-15 MeV	1.6 m	1 TW	1 klystron 20 MW	2856 MHz	0.6×10^{-3}	10 mA to 1.5 A for 4 μ sec pulses 10 mA to 1.5 A for 10 nsec pulses	Flexible repetition rate (1-200 pps) Very short high current pulses Very low attenuation ~ 0.125 meters Special H.V. retards with 200 kV between cathode and anode 5% spectrum for 1.3 A pulse 80% conversion efficiency

all operate at S-band in the neighborhood of 3000 MHz. Most of the machines came into operation after 1960 and have been upgraded in some way since their inception. One of the noteworthy features is the trend toward higher current pulses, both in the nanosecond and microsecond range. This, in the case of some of the longer accelerators, has necessitated more focusing and HEM₁₁-mode detuning to control beam breakup (BBU). As an example, with these and other improvements, the Kharkov 2 GeV linac, now limited to 1.5 GeV because of RF breakdown problems, may gradually be upgraded¹³ to produce 3 μ s, 100 mA pk pulses at 2 GeV. In addition, this machine is presently being fitted with a polarized electron source based on elastic electron-hydrogen spin-exchange collisions.¹⁴

Another noteworthy innovation is the development and installation of energy compression systems (E.C.S.), first at Mainz and now at Tohoku and Glasgow. This system was first tried by M. Crowley-Milling and G. Saxon¹⁵ at NINA. It is based on using a non-isochronous achromatic magnet system to debunch a beam emerging from the accelerator with a poor spectrum and then compressing the spectrum by passing the electrons through an accelerating structure in phase quadrature with the other sections. With a "linear" ramp (which can be improved by adding a second harmonic cavity as proposed by the group at Glasgow), a lower-energy electron which has been retarded will receive a positive energy, and vice versa, a higher-energy electron which has been advanced will receive a negative energy. At Mainz, where the system has been in operation since 1972, a compression factor of 7 from $\Delta E/E$ of 1% down to 0.14% has been obtained.

b. Special Medium-Energy High Duty Cycle Machines

By the time the Medium Energy Accelerator (MEA) at IKO, Amsterdam, comes into operation (140 MeV in 1977, full 530 MeV in 1979), it will be the third machine in this class, together with the ALS linac at Saclay and the Bates linac at MIT. Since these accelerators have been described in great detail in the recent literature,^{16,17,18} only their main parameters are summarized for comparison in Table VI. All three machines are or will be devoted to electron scattering, pion and muon physics. Narrow energy spectrum and small emittance are at a premium to permit optimum use of their spectrometers, some of which have momentum resolutions $\Delta p/p$ in the range 10^{-4} to 10^{-5} .

Recent work at the ALS includes extensive use of beam switching among experimenters and computer-aided

operation described in a separate paper by G. Bianchi et al. at this conference. The machine is now equipped with a positron source with a power-handling capability of 3-5 kW to be upgraded to 20 kW. With a 200 μ A average current of 85 MeV electrons incident on a gold target, it should produce a positron current of 200 nA average.

The Bates linac is now in steady operation. Work continues on improving their modulator switch tubes whose MTBF has now reached 7000-8000 hours. At IKO, installation is proceeding. Recent tests with their klystrons and solid-state modulators have produced¹⁹ 500 pps with a pulse length of 50 μ s at 1 MW peak power. Voltage ripple is within 1%. Injector beam tests are under way.

c. The Next Step for High Duty Cycle Machines

Beyond the medium-energy high duty cycle linacs just discussed lies a major challenge to the accelerator community. A number of discussions have been held in the last few years in the USA and elsewhere to ascertain what the next step should be. While there cannot be unanimous agreement on the beam parameters before the type of accelerator is actually chosen, we might for the sake of discussion set our minds on a 1 GeV, 100 μ A CW machine. To achieve such parameters, there are today at least six possible candidates:

1. a conventional CW "brute force" linac
2. a conventional CW linac with recirculation
3. a multistage racetrack microtron
4. a pulsed linac with a beam stretcher
5. a superconducting linac
6. a superconducting linac with recirculation.

Let us consider these briefly. A CW linac would make use of a standing-wave structure with a good shunt impedance, say 67 M Ω /m, at S-band. Higher shunt impedances could indeed be considered, as mentioned earlier in this paper, but probably at the expense of reducing the central iris diameter to a dimension unsafe for this application, particularly if beam recirculation must be considered. CW klystrons with 500 kW output power are now available and, while quite expensive, may come down in price below \$100K if ordered in quantity. Assuming a gradient of 1.66 MV/m and a length of 600 m, one would need fifty 500 kW klystrons. The RF structure would have to be able to dissipate about 40 kW/m, which is high but does not look impossible. Taking beam centerline costs (including accelerator sections, supports, vacuum and waveguides, but no instrumentation or

Table V: Conventional low- and medium-energy electron linacs for nuclear physics.

Institution	Maximum Energy (MeV)	Maximum Peak Current (mA)	Beam pulse length (μsec) / Repetition rate (pps)	Beam Duty Cycle	Number and Peak Power of Klystrons	Total Accelerating Length (m)	Special Features
Centro Atomico Bariloche, Argentina	25	300	1.2 / 200	2.4×10^{-4}	1 / 15 MW	3	
IFK, Darmstadt, Germany	70	60	5 / 150	7.5×10^{-4}	1 / 22 MW	6.6	Energy loss spectrometer
LVK, Gent, Belgium	90	400	3 / 300	9×10^{-4}	2 / 20 MW	6	BBU at 400 mA, 3 μsec e ⁺ source u.c. ^a
IFK, Giessen, Germany	65	400	2 / 250	5×10^{-4}	1 / 30 MW	8	e ⁺ source u.c. ^a
U. of Glasgow, UK	130	300	3.5 / 240	8.4×10^{-4}	3 / 25 MW	18	BBU at 300 mA, 3.5 μsec E.C.S. ^b u.c. ^a
U. of Glasgow, UK	30	>500	3.5 / 240	8.4×10^{-4}	1 / 25 MW	3.5	
Harwell, UK	55	500	2 / 200	4×10^{-4}	7 / 8 MW	~20	
Harwell, UK	136	1000	5 / 300	1.5×10^{-3}	8 / 20 MW	~24	L-Band
KhFTI, Kharkov, USSR	280	15	1.5 / 50	7.5×10^{-5}	11 / 14 MW	~48	
KhFTI, Kharkov, USSR	1500	25	1.5 / 50	7.5×10^{-5}	51 / 14 MW	~225	{ e ⁺ source in existence Polarized electron source u.c. ^a Overall improvement plan under consideration.
IFK, Mainz, Germany	350	250	4 / 150	6×10^{-4}	8 / 23 MW	~40	E.C.S. ^b
NPCS, Monterey USA	110	25	1 / 60	6×10^{-5}	3 / 20 MW	9	
RTI, Moscow, USSR	60	1000	5.5 / 50	2.7×10^{-4}	6 / 25 MW	~20	Long high current pulses
RTI, Moscow, USSR	30	10000	0.01/2400	2.4×10^{-5}	1 / 30 MW	~8	Nanosecond high current pulses
Oak Ridge, USA	178	20000	0.024/1000	2.4×10^{-5}	4 / 30 MW	16.5	L-Band Nanosecond high current pulses
NRC, Ottawa, Canada	35	250	3.2 / 180	6×10^{-4}	1 / 20 MW	8	
CBPF, Rio de Janeiro, Brazil	30	100	3.3 / 360	1×10^{-3}	2 / ?	~10	1 Amplatron, 1 Klystron
IDF, São Paulo, Brazil	50	10	1 / 120	1×10^{-4}	2 / 21 MW	~6	
U. of Saskatchewan, Canada	280	300	1 / 360	3.6×10^{-4}	6 / 22 MW	20	Pulse stretcher "EROS" proposed
U. of Tohoku, Sendai, Japan	380	120	3 / 300	9×10^{-4}	5 / 20 MW	54	BBU at 35 mA, 3 μsec. E.C.S. ^b
HEPL, Stanford, USA	1200	30	1.3 / 120	1.6×10^{-4}	31 / 20 MW	93	No longer operable at max energy
JAERI, Tokai, Japan	190	350	2 / 150	3×10^{-4}	5 / 20 MW	13	
NBS, Washington, USA	150	350	5 / 360	1.8×10^{-3}	12 / 5 MW	30	L-band, BBU at 200 mA, 5 μsec Can generate short 5A pulses
Yale University, USA	70	750	4.5 / 200	9×10^{-4}	5 / 10 MW	15	L-band, can generate short 10A pulses

^au.c. : under construction

^bE.C.S. : Energy compression system

Table VI: Comparison of main parameters of medium energy high duty cycle machines.

Name	SACLAY ALS	MIT BATES	KO MEA (under construction)
Maximum design energy and beam duty cycle	600 MeV 1% 470 MeV 2%	430 MeV 1.8% 200 MeV 5.6%	400-500 MeV 2% 250-400 MeV 4% 200-250 MeV 8%
Beam pulse repetition rate and length ^a	3000 pps (max) 20 μ sec (max)	5000 pps (max) 13 μ sec (max)	2000 pps (max) 45 μ sec (max)
Current	42 mA pk (max) 370 μ A av (max)	25 mA pk (max) 250 μ A av (max)	20 mA pk (max) 500 μ A av (max)
Energy spectrum	5mA pk at 1000 pps within $\frac{\Delta E}{E} = .1\%$	85% of current within $\frac{\Delta E}{E} = .3\%$	50% of current within $\frac{\Delta E}{E} = .3\%$
Output emittance	90% of current within $0.01\pi \left(\frac{\text{MeV}}{c}\right) \text{cm}$	90% of current within $0.0006\pi \left(\frac{\text{MeV}}{c}\right) \text{cm}$	90% of current within $0.006\pi \left(\frac{\text{MeV}}{c}\right) \text{cm}$
Recent beam-hours per year	4000	4000	---
Number and peak power of klystrons	15 / 4 MW pk	10 / 4 MW pk	12 / 4 MW pk
Accelerating length	~ 170 m	~ 153 m	~ 180 m

^a The maxima given here are extrema and cannot be reached together.

building costs) at \$25K/m and 1 MW regulated power supplies at \$100K, the cost of the klystrons, power supplies, and the accelerator would amount to \$25M. The total power demand of 50 MW would seem prohibitive and hard to justify, especially since the beam power would be only 100 kW at 100 μ A. (Actually, the beam current could easily be increased to 1 mA and would still only contribute 48 MeV of beam loading.) Given these facts, one is forced to think in terms of at least one, two, or three turns of recirculation.²⁰ With the same klystrons as above, all the above numbers are then reduced by 1/n where n is the total number of passes, except for the average current present in the accelerator, which is multiplied by n. The risk of beam breakup probably increases²¹ as n^2 but the effect should be controllable with focusing and possibly feedback. Thus with 4 passes the accelerator might only be 150 m long, use ~13 klystrons, and require ~13 MW of power. The above cost, even allowing \$3-4M for the recirculation system, might come down by a factor of 2.

The next candidate to consider is the multistage or cascaded racetrack microtron. A feasibility study for such an accelerator of up to 820 MeV and 100 μ A with 3 stages (14, 100, and 820 MeV) has been carried out at Mainz, Germany.²² The cost is estimated at \$3M. A total of seven 50 kW klystrons would be needed. Specific magnets and RF components are presently under investigation. Final feasibility remains to be proven and careful beam breakup calculations must still be made. The advantage of this project, however, is that the three stages can be built sequentially and resources can be committed gradually as each stage is proven to perform successfully.

We now come to the pulsed linac followed by a beam stretcher. Combinations of this type have already been studied for the ALS (600 MeV) and the University of Saskatchewan (250 MeV) linacs (Projects ALIS²³ and

EROS²⁴). One of the problems in designing a satisfactory stretcher is to be able to extract a beam with a small phase space and a narrow energy spectrum. In our case, one might start with a 1 GeV, 100 μ A average, 200 mA peak current linac. With a 10^{-3} RF duty cycle, 36-MW klystrons and 2-meter sections with an attenuation of 0.2 nepers, such an accelerator would have to be 60m long and have 30 klystrons. As an example, a stretcher with a 26m radius could be filled in a single orbit time of 500 ns. The linac RF pulse length could be ~1 μ s, i.e., ~0.3 μ s for the linac filling time and 0.7 μ s for the beam pulse, of which the last 0.5 μ s would be used for injection. The repetition rate would be 1000 pps. Each pulse would contain at least 6×10^{11} electrons within an energy spectrum of 0.5%. The electrons outside of this range would be lost in momentum defining slits. Injection into the stretcher could be achieved on-orbit in slightly less than one turn followed by resonant extraction and uniform spillage in the interpulse period of about 1 ms. Transient beam loading in the linac would be

of the order of 50 MeV (5%) but it could be significantly reduced by staggered triggering of successive klystrons. The energy lost through synchrotron radiation in the stretcher would be 3.40 keV per turn or 7 MeV for the entire storage time. The details of the extraction system and resultant phase space of the spilled beam would have to be studied in detail. The cost of the linac might be of the order of \$9M and the stretcher \$3M.

Finally, let us consider the solution using a superconducting linac under (5) and (6). To do this, we must review briefly the status of RF superconducting work relevant to electron linacs. Low frequency helix and split-ring structures of the type proposed for proton and ion accelerators are covered elsewhere at this conference.

If we look at the evolution of this field in the last five years, we see that significant progress has been made in exploring and understanding some of the existing difficulties, that a number of new ideas and techniques have been explored, but that no major breakthrough has yet occurred. Indeed, much has been learned about Niobium surfaces, their treatment, defects, thermal and magnetothermal breakdown, hot spots, and multipactoring.²⁵ Activities at Cornell,²⁶ Illinois,²⁷ Stanford,²⁸ and Karlsruhe²⁹ are summarized in Table VII. New work on Nb₃Sn is also being done at Siemens³⁰ and Wuppertal,³¹ as well as at Karlsruhe.³²

From these numerous references, one can draw the following conclusions:

(i) The extremely high effective gradients, i.e., 30 MV/m, that had been hoped for a few years ago do not seem practicable with presently known materials. Q_0 's of $\sim 10^9$ and $E_{\text{eff}} \sim 2-3$ MV/m are attainable in actual L- and S-band Niobium structures at 1.8°K when proper surface treatment techniques are used. These

Table VII: Summary of major activities relevant to superconducting electron linacs.^a

Institution	Cornell	Illinois	Stanford	Karlsruhe
Main Project	RF structures for synchrotrons and storage rings	Racetrack microtron	Recyclotron	RF separators for CERN (proton and heavy-ion accelerators not treated here)
RF structures	2856 MHz rectangular "Muffin-Tin" 1, 2, 6 cells, solid and pressed Nb sheet	1300 MHz HEPL $3 \lambda/2 + 13 \lambda/2$ Nb	1300 MHz $3-4 49\lambda/2$ Nb	2865 MHz Two 0.6 m prototypes Two 2.74 m final models $\pi/2$ mode, 104 cells each Nb
Best practical RF results obtained	$Q_0 = 6 - 14 \times 10^9$ $E_{\text{eff}} = 6.9 \text{ MeV/m}$ at $1.4 - 2.2^\circ\text{K}$	$Q_0 = 10^7 - 10^8$ $E_{\text{eff}} = 4 \text{ MeV/m } 50\% \text{ D.C.}$ at 4.2°K	$Q_0 \sim 10^9$ $E_{\text{eff}} = 2 \text{ MeV/m } 100\% \text{ D.C.}$ $E_{\text{eff}} = 3 \text{ MeV/m } 10\% \text{ D.C.}$ at 1.9°K	$Q_0 = 9 \times 10^8$ $E_{\text{eff}} = 2 \text{ MeV/m}$ in prototype $E_{\text{eff}} = 1.2 \text{ MeV/m}$ in sections of final model at 1.8°K
Beam operation	Structure used in Cornell synchrotron, electrons accelerated to 4 GeV	MUSL-I with 6 passes has routinely produced 19 MeV, $5 \mu\text{A}$ cw electrons	Injector: 7 MeV First pass: 47 MeV, $500 \mu\text{A}$ $10\% \text{ D.C.}$ 24 MeV, $50 \mu\text{A}$ $100\% \text{ D.C.}$ Second pass: 70 MeV, $15 \mu\text{A}$	Scheduled for future use on SPS at CERN
Difficulties and problems to be solved	- Light spots, possibly incandescent dust particles - Hot spots, studied with carbon resistor thermometers - Accelerating field not uniform over aperture	- Possible beam breakup - Relative phasing of sections - Orbitry	- Magnetothermal breakdown: surface defects limit critical field to 100-300 Oe - Multipactoring - Possible beam breakup	- Occasional magnetothermal breakdown and multipactoring - Localized light spots with light intensity proportional to RF power in all but one mode
Other associated projects and future plans	- Nb sputtering - Nb_3Sn experiments - Understanding of multipactoring - X-band multi-cell structures	MUSL-II using $49 \lambda/2$ HEPL structure and 3 GeV VdG injector Goal: 60 MeV with 6 passes, $30 \mu\text{A}$, $100\% \text{ D.C.}$	- Stabilization of surfaces - Study of multipactoring trajectories - Build up to 4 orbits, 225 MeV, $100 \mu\text{A}$, $100\% \text{ D.C.}$	- New sequence in Nb surface treatments and final assembly, August 1976 - Final tests - Shipment to CERN hoped for early 1977

^aOther important work carried out at Siemens and Wuppertal in Germany is referred to in the text.

treatments and what is considered optimum seem to vary from one laboratory to another. The above gradients have been exceeded in a number of cases such as the "Muffin-Tin" structure (see Fig. 5) at Cornell, but reliability and reproducibility on a large scale remain uncertain.

(ii) The critical magnetic field H_{c1} for Type-II superconductors such as Niobium which was believed to be the level above which "quenching" occurs has been shown not to be the upper limit. On the other hand, the surface defects in Niobium which lead to magneto-thermal runaway seem to have a finite probability of occurring even when all the best polishing and thermal surface treatment techniques are applied. Thus, the larger the surface, the larger the probability of failure, and hence there is a trend toward favoring higher frequencies (S- and perhaps even X-band) for which the objects to be manufactured are smaller.

(iii) Similarly, field emission and multipactoring continue to occur, particularly at L- and S-band. Multipactoring electrons deliver energy to the superconducting surface and can drive it normal. They can also provide a non-linear coupling mechanism between the accelerating field and other cavity modes, thereby affecting beam energy. While multipactoring can often be reduced by careful RF

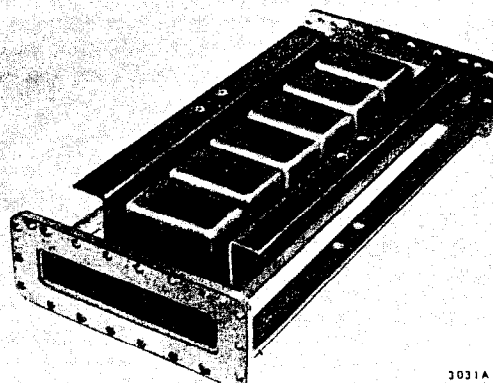


Fig. 5--Cornell "Muffin-Tin" slow-wave structure made out of pressed Niobium sheet.

processing, it has a tendency to reappear at other operating levels, thereby impairing flexible operation.

Another limiting phenomenon which may or may not be related to multipactoring has appeared at Cornell and Karlsruhe in the form of light emitting spots. These could result from incandescent impurities but they are not well understood.

(iv) Very active work continues on the search for better materials. As pointed out in Ref. 30, if H_c is no longer a limit, one may benefit by going to one of the A15 compounds such as Nb_3Sn with a higher critical temperature T_c . Such a choice, if Nb_3Sn can be used at 4.2°K, would result in lower refrigeration costs and possibly more stable surfaces. Here again, a higher frequency would be favored because the residual surface resistance which is not temperature-dependent dominates at lower frequencies and does not make it worthwhile to improve the so-called BCS surface resistance which depends on T as well as frequency.

As indicated in Table VII, a second pass of the beam has been successfully attempted at Stanford and work is proceeding to obtain up to four orbits and an energy up to 225 MeV. This program is promising but it is not straightforward. Problems associated with beam break-up, extraction, reinjection, and reliability still remain to be shown solvable on a routine basis to make such an accelerator usable for physics research. Furthermore, costs of superconducting structures are still very high (numbers of the order of \$40K/m are being quoted) and further effort such as the work at Cornell will be needed to bring these down.

Thus, to conclude, superconductivity may some day provide an answer to our 1 GeV, 100 μ A CW accelerator, but at 2 MeV/m it will not be a short machine and, most probably, it will require recirculation. In any case, several years of steady work are still needed. Choosing among our six proposed alternatives will depend greatly on when the choice has to be made.

d. Injectors into Synchrotrons and Storage Rings

There are today at least five conventional electron synchrotrons which use a linac as an injector: the University of Tokyo I. N. S. 1.3 GeV synchrotron with a 15 MeV linac, the Bonn 2.5 GeV synchrotron with a 20 MeV linac, the Yerevan 6.1 GeV synchrotron with a 50 MeV linac, the Cornell 12 GeV synchrotron with a 150 MeV linac, and possibly the Tomsk 1.5 GeV synchrotron (insufficient information). All these linacs produce only electrons, and fairly straightforward injection techniques are used to optimize the match between linac and synchrotron RF frequencies.

Similarly, a new 15 MeV linac is presently on order from the Radiation Dynamics Corp. for injection into the future Daresbury* S. R. S. synchrotron light facility and a 2.5 GeV linac is under design for the proposed KEK Photon Factory in Japan. The machines which pose a greater challenge to the accelerator designer are those which must generate electrons as well as positrons for injection into e^\pm storage rings. Table VIII

*The NINA synchrotron at Daresbury will be de-commissioned shortly.

summarizes performance characteristics of the e^\pm injectors presently in existence. The e^- injection performance is not given in the table because in most cases it is much easier than for e^+ , or, as in the case of DESY, it is achieved with a separate linac. Making a comparison between the various modes of injection is not necessarily meaningful because of the differences in ring RF frequencies, energies of e^- incident on e^+ target, focusing systems, etc. Thus the absolute number of positrons producible per second varies greatly from one machine to another. What is interesting, however, is to notice that in spite of this large diversity of conditions, the average e^+ current per kilowatt of e^- beam incident on the source does not vary greatly. This result is not very surprising because all targets and e^+ focusing systems resemble each other and no major breakthrough has recently been made. What will be valuable in the future is the feature now available at SLAC up to 2.5 GeV to "top-off a given fill", namely to refill the ring at the energy at which it is doing physics without first dumping the remaining charge which in the past was judged insufficient to continue to run. At energies where this "topping-off" mode has been usable, the average operating luminosity of the ring was recently doubled. Further improvements to upgrade e^+ yield and capture, and to speed up the switching time between e^+ and e^- filling are very much in demand, particularly for future storage rings such as PEP.

e. Multi-GeV Linacs

By our definition, the only electron linac in this category is the SLAC 3-km accelerator. Fifteen years ago, when construction of SLAC was beginning, it was not as unlikely as it is today that a yet higher-energy electron linac would some day get funded and built. In the meantime, proton synchrotrons have proven to be more practicable and economical at higher energies, and electron and proton storage rings now hold the promise of much higher center-of-mass energies. There has recently been some discussion at CERN regarding the feasibility of multi-GeV colliding "linear" beams using collinear superconducting linacs but, with the presently available gradients (2-3 MeV/m), such machines would be unacceptably long and expensive. At SLAC, over the past ten years, there have been proposals to (a) double or quadruple the number of klystrons, thereby multiplying the present energy by $\sqrt{2}$ or 2, (b) convert the present copper accelerator sections to superconducting Niobium structures, thereby obtaining a CW 100 GeV beam (now very unlikely), and (c) recirculate the 20 GeV beam for

Table VIII: Performance characteristics of the present e^\pm linac injectors for colliding beam facilities.

Machine and location	Energy of e^- incident on e^+ target	e^- beam power incident on target while injecting	Target material	Nanoamps of e^+ within $\Delta E/E = 1\%$ per kW of incident e^- beam	Energy of e^+ at output of linac
ADONE Frascati	80 MeV	< 1 kW	Copper	9.4	380 MeV
DESY-DORIS Hamburg	320 MeV	~ 1 kW	Tungsten	15	320 MeV
DCI Orsay	~ 1 GeV	< 1 kW	Tungsten	7.1	1.2 GeV (max)
SLAC-SPEAR Stanford	~ 6 GeV	< 1 kW	Tungsten-Rhenium	11.1	2.5 GeV (max)
ALS ^a Saclay	85 MeV	3 kW	Gold	13.4	~ 500 MeV

^a Not an injector for storage rings, listed for comparison only.

a second pass up to 40 GeV (Project RLA). All these proposals were successively abandoned because of high cost and/or technical difficulties. On the other hand, the project which has not only been approved but is now under installation is SLED (for SLAC energy development). The principle of this idea has been amply described in the literature.^{33,34} The potential of SLED is to increase the present SLAC energy by a factor of ~ 1.4 (Stage I) with the existing $2.7 \mu\text{s}$ RF pulse length at 360 pps, and later by a factor of ~ 1.8 (Stage II) through conversion to $5 \mu\text{s}$ RF pulses at 180 pps (leaving total AC power constant). The progression of Stage I construction and installation which is under way at the present time is summarized in Table IX. Its rate of completion is contingent on funding assumptions outlined in column 3. Beam performance with two sectors (out of 30) installed has already been verified

and is shown in Fig. 6. The energy contribution measurements were made with a 30 ns, 5 mA beam pulse that could be moved in time through the RF pulse. Under actual operation, the beam pulse length will be between 200 and 300 ns and the current amplitude will be tailored so that beam loading compensates for the energy rise inherent in the theoretical curve shown in Fig. 6, and thereby yields an energy spectrum $\Delta E/E$ as narrow as possible. Peak currents of up to 150 to 200 mA will be needed. It has been shown experimentally as well as theoretically that values above 110 mA cannot presently be attained because of beam breakup. Thus additional quadrupole focusing along the accelerator is being planned. The increase in operating energy up to 32 GeV will also require upgrading the present capability of the beam switchyard magnets. This program is under way.

Table IX: SLED Stage I ($2.7 \mu\text{s}$ RF pulses).

Assumptions	Maximum no-load energy without SLED : 23 GeV
	Peak klystron power : 24 MW ^a
	Present maximum peak current : 50 mA or 50×10^{10} e ⁻ /pulse at 1.6 μs delivered to experimenters
	Repetition rate : 360 pps
	Duty cycle with 230 ns pulses : 8.2×10^{-5}

Increment	Cumulative Number of Sectors	Funding Assumptions ^{b/}	Cumulative no-load Energy Increment GeV	Total Energy With Beam Loading GeV	Pulse Length ns	Current Within 1% spectrum mA peak	e ⁻ /pulse	Completion Date
1	3	Feb. 75 \$600K	1.01 ^{c/}	23.77	230	14.7	2.2×10^{10}	Sept. 76
2	11	Dec. 75 \$1200K	3.71	25.82	230	54	7.8×10^{10}	July 77
3	18	Oct. 76 \$1050K	6.07	27.61	230	88.4	12.7×10^{10}	Nov. 77
4	30	Oct. 77 \$2810K	10.12	30.68	230	147	21.8×10^{10}	Sept. 78

^{a/} The 24 MW figure is an effective average number resulting from the present klystron population mix :

24 ~ 40 MW tubes
70 ~ 30 MW tubes
150 ~ 20 MW tubes

^{b/} The funds given in this column are to cover the SLED cavity installation program, new pulsed focusing along the accelerator to control beam breakup and beam switchyard improvements to accommodate the higher energy beams.

^{c/} This number corresponds to a no-load energy increment of 0.336 GeV per sector. Installation and testing of the first two SLED sectors as of July 1976 have made it possible to confirm this number experimentally.

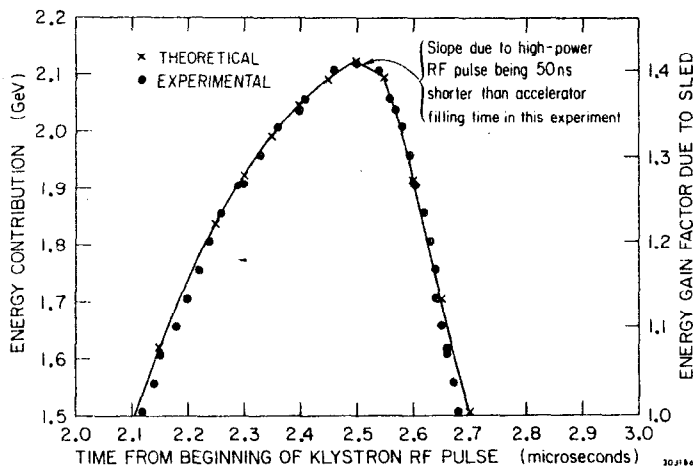


Fig. 6--Energy contribution of two SLAC sectors (Nos. 16 and 17) with SLED cavities installed, as a function of time within pulse.

Besides the SLED program, there are many other ongoing linac developments at SLAC. Limited space does not allow us to describe them in extensive detail but a few can be mentioned briefly. In the past three years, a polarized electron source³⁵ based on ionizing polarized Lithium atoms with a pulsed flash-lamp has been developed successfully. It can deliver peak currents of $300 \mu\text{A}$ to the switchyard with 85% polarization. Another source using circularly polarized laser light incident on a Gallium Arsenide photocathode is presently under construction. Its goal is to produce peak currents of at least 20 mA with 50% polarization. In another area, beam loading studies have been carried out to measure the energy loss of single bunches to higher-order microwave modes.³⁶ Instrumentation and computer control developments have been numerous. Up to eight interlaced beams with different currents and energies can now be generated and used with great flexibility. New beam position monitors³⁷ have been developed which can detect beam centroid displacements down to $10 \mu\text{m}$ at peak currents of $100 \mu\text{A}$. Microprocessors are beginning to appear in a variety of applications such as the klystron phasing and trigger systems. Further

developments are on the horizon to make the linac more responsive to the needs of the present storage ring SPEAR and the future ring of PEP.

Finally, it seems worthwhile mentioning the research of Professor R. H. Pantell at Stanford University on electron acceleration by lasers. The basic idea which was initially tested on the Mark III linear accelerator at the W. W. Hansen Laboratories³⁸ will soon be the subject of an experiment by the same group with the 6-MeV test accelerator at SLAC. The principle is to shoot this 6-MeV electron beam alongside a 2 MW, 10 ns laser pulse into a chamber with 10 Torr Na gas. The laser direction of incidence is at the Cerenkov angle with respect to the beam so that there is cumulative acceleration of the electrons due to synchronism with the E-field projection along their direction of motion. Work on this project is in its infancy but could be very promising for certain applications.

Acknowledgements

The author wishes to thank the fifty or so colleagues who so diligently and painstakingly filled out the questionnaire which he mailed them, the answers to which supplied him with a sizable fraction of the information contained in this paper. He also wishes to acknowledge useful discussions with M. Bagshaw, P. Brunet, J. Conforti, P. Demos, P. Fessenden, J. Haimson, J. Halbritter, C. Karzmark, E. Knapp, H. Lengeler, C. Lyneis, R. Miller, F. Netter, C. Nunan, T. Smith, W. Swanson, M. Tigner, W. Turchinets, and P. Wilson.

References

1. R. Loevinger, C. J. Karzmark, and M. Weissbluth, *Radiology* 77, No. 6, 906 (Dec 1961).
2. This list is fairly complete but may not be exhaustive. It was compiled from information sent to the author by the manufacturers and a similar list made by Dr. C. J. Karzmark at the Stanford University Medical Center, Stanford, California.
3. E. A. Knapp, LASL, private communication. See also S. O. Schriber, L. W. Funk, R. M. Hutcheon, "Effective Shunt Impedance Comparison between S-band Standing Wave Accelerators with On-axis and Off-axis Couplers," paper presented at this conference.
4. Henry S. Kaplan, H. Alan Schwettman, William M. Fairbank, Douglas Boyd, Malcolm Bagshaw, *Radiology* 108, No. 1, 159 (July 1973).
5. J. N. Bradbury, E. A. Knapp, and D. E. Nagle, *IEEE Trans. Nucl. Sci.* NS-22, No. 3, 1755 (June 1975).
6. J. Haimson, B. Mecklenburg, *IEEE Trans. Nucl. Sci.* NS-22, No. 3, 1805 (June 1975).
7. Perry B. Wilson and Craig S. Nunan, *IEEE Trans. Nucl. Sci.* NS-20, No. 3, 1018 (June 1973).
8. D. Boyd, P. Fessenden, and G. Luxton, private communication.
9. R. B. Neal, ed., *The Stanford Two-Mile Accelerator* (W. A. Benjamin, New York/Amssterdam, 1968).
10. This table was compiled from information sent to the author by the manufacturers and a similar table made by Dr. W. P. Swanson at SLAC.
11. J. Haimson, B. Mecklenburg, and V. Valencia, *IEEE Trans. Nucl. Sci.* NS-22, No. 3, 1303 (June 1975).
12. J. Haimson, *IEEE Trans. Nucl. Sci.* NS-22, No. 3, 1354 (June 1975).
13. V. A. Vishnyakov, private communication.
14. V. P. Efimov, I. M. Karnaukov, and V. A. Vishnyakov, *On the Problem of Polarized Beam Formation at the 2 GeV Electron Linac*, *Fisiko-Tekhnicheskii Institut an USSR, Voprosi Atomnoi Nauki i Tekhniki*, Seriya : Lineie Uskoriteli, Vipusk 1 (1), KhFTi 75-6 (Kharkov, 1975), p. 11.
15. M. C. Crowley-Milling and G. Saxon, *The Use of a Debuncher in the Injection Path of an Electron Synchrotron*, *Daresbury Nuclear Physics Laboratory Report DNPL/R16* (1971).
16. See for example J. Haimson, "High Duty Factor Electron Linear Accelerators," in *Linear Accelerators*, ed. Lapostolle and Septier (North Holland Publishing Co., Amsterdam, 1970), p. 415; J. Haimson, *IEEE Trans. Nucl. Sci.* NS-20, No. 3, 914 (June 1973); or C. Sargent, W. Turchinets, J. Weaver, *IEEE Trans. Nucl. Sci.* NS-22, No. 3, 1341 (June 1975).
17. P. Bruinsma, E. Heine, G. Koenderink, and J. van Koeverden Brouwer, *IEEE Trans. Nucl. Sci.* NS-20, No. 3, 365 (June 1973).
18. IKO Annual Report 1975, p. 59.
19. P. Bruinsma, private communication.
20. A study to recirculate the beam from the Bates linac up to 750 MeV for a second pass is actually under way (P. Demos, private communication). Similarly, there is a design project at the Yerevan Physical Institute to build and then recirculate a 120 MeV, 0.2 A pulsed linac beam up to 240 MeV. See Yu. G. Basargin et al., *A High Current Electron-Positron Linac with a Reaccelerated Electron Beam*, *Fisiko-Tekhnicheskii Institut an USSR, Voprosi Atomnoi Nauki i Tekhniki*, Seriya : Lineie Uskoriteli, Vipusk 1 (1), KhFTi 76-19 (Kharkov, 1976), p. 7.
21. V. Volodin and A. Hanson, *IEEE Trans. Nucl. Sci.* NS-22, No. 3, 1194 (June 1975).
22. H. Herminghaus, A. Feder, K. Kaiser, W. Manz, and H. V. D. Schmitt, "The Design of a Cascaded 800 MeV Normal Conducting C.W. Race Track Microtron," submitted to *Nucl. Instrum. Methods* (June 1976).
23. R. Beck et al. in *Proc. Int. Conf. on High Energy Accelerators*, Yerevan, 1969 (*Acad. Sci. ASSR*, Yerevan, 1970), Vol. 2, p. 94.
24. N. Heese and R. Servranckx, *Proc. IXth Int. Conf. on High Energy Accelerators*, Stanford, 2-7 May 1974, ed. R. B. Neal, p. 618.
25. H. Schwettman, *IEEE Trans. Nucl. Sci.* NS-22, No. 3, 1118 (June 1975).
26. H. Padamsee et al., "Fabrication and Performance of 'Muffin-Tin' Microwave Cavities for Accelerator Use," paper presented at the 1976 Applied Superconductivity Conference, Stanford, 17-20 Aug 1976.
27. P. Axel, A. Hanson, J. Harlan, R. Hoffswell, D. Jamnik, D. Sutton, L. Young, *IEEE Trans. Nucl. Sci.* NS-22, No. 3, 1176 (June 1975).
28. T. Smith, (Stanford) *High Energy Physics Laboratory Report HEPL 778* (1976).
29. A. Citron, G. Dammert, M. Grundner, L. Husson, P. Kneisel, H. Lengeler, and E. Rathgeber, "Progress on the Superconducting RF-Particle Separator for CERN," paper presented at the 1976 Applied Superconductivity Conference, Stanford, 17-20 August 1976.
30. B. Hillenbrand, H. Martens, H. Pfister, K. Schnitzke, and Y. Uzel, "Superconducting Nb₃Sn Cavities with High Microwave Qualities," paper presented at above conference (see Ref. 29).
31. G. Arnolds, D. Proch, "Measurement on a Nb₃Sn Structure for Linear Accelerator Application," paper presented at above conference (see Ref. 29).

32. P. Kneisel, H. Küpfer, W. Schwarz, O. Stoltz, and J. Halbritter, "On Properties of Superconducting Nb₃Sn used as Coatings in RF Cavities," paper presented at above conference (see Ref. 29).
33. Z. D. Farkas, H. A. Hogg, G. A. Loew, and P. B. Wilson, Proc. IXth Int. Conf. on High Energy Accelerators, Stanford, 2-7 May 1974, p. 576.
34. Z. D. Farkas, H. A. Hogg, G. A. Loew, and P. B. Wilson, IEEE Trans. Nucl. Sci. NS-22, No. 3, 1299 (June 1975).
35. M. J. Alguard et al., Stanford Linear Accelerator Report No. SLAC-PUB-1789 (1976).
36. R. F. Koontz, "Single-Bunch Beam Loading on the SLAC Two-Mile Accelerator," Stanford Linear Accelerator Center Report No. SLAC-195 (1976).
37. Z. D. Farkas, H. A. Hogg, H. L. Martin, and A. R. Wilmunder, "Recent Developments in Microwave Beam-Position Monitors at SLAC," paper presented at this conference.
38. M. A. Piestrup, G. B. Rothbart, R. N. Fleming, and R. H. Pantell, J. Appl. Phys. 46, 132 (1975).